Accepted Manuscript

Aptamer induced multicoloured Au NCs-MoS_2 "switch on" fluorescence resonance energy transfer biosensor for dual color simultaneous detection of multiple tumor markers by single wavelength excitation

Shenghao Xu, Xiuying Feng, Teng Gao, Gufan Liu, Yaning Mao, Jiehua Lin, Xijuan Yu, Xiliang Luo

PII: S0003-2670(17)30729-8

DOI: 10.1016/j.aca.2017.06.023

Reference: ACA 235271

To appear in: *Analytica Chimica Acta*

Received Date: 26 March 2017

Revised Date: 2 June 2017

Accepted Date: 7 June 2017

Please cite this article as: S. Xu, X. Feng, T. Gao, G. Liu, Y. Mao, J. Lin, X. Yu, X. Luo, Aptamer induced multicoloured Au NCs-MoS_2 "switch on" fluorescence resonance energy transfer biosensor for dual color simultaneous detection of multiple tumor markers by single wavelength excitation, *Analytica Chimica Acta* (2017), doi: 10.1016/j.aca.2017.06.023.

Graphical Abstract

Aptamer induced multicoloured Au NCs-MoS2 "switch on" fluorescence resonance energy transfer biosensor for dual color simultaneous detection of multiple tumor markers by single wavelength excitation

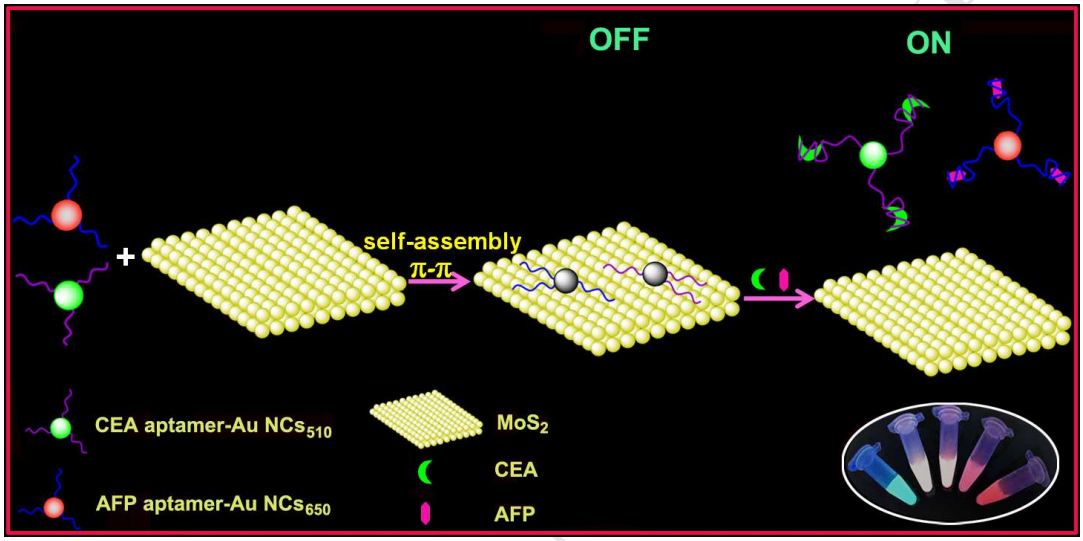

A novel fluorescent "switch on" FRET-based aptasensor for simultaneous detection of multiple tumor markers (dual colored Au NCs as energy donors and MoS_2 nanosheets as acceptors) with a single excitation was developed for the first time.

Aptamer induced multicoloured Au NCs-MoS2 “switch on” fluorescence resonance energy transfer biosensor for dual color simultaneous detection of multiple tumor markers by single wavelength excitation

Shenghao Xu,[a] *Xiuying Feng,*[a] *Teng Gao,*[a] *Gufan Liu,*[a,b] *,Yaning Mao,*[a] *Jiehua Lin,*[a] *Xijuan Yu*[a] *and Xiliang Luo,**[a]

[a]Key Laboratory of Sensor Analysis of Tumor Marker Ministry of Education, College of Chemistry and Molecular Engineering, Qingdao University of Science and Technology, Qingdao 266042, P. R. China

[b] College of Polymer Science and Engineering, Qingdao University of Science and Technology, Qingdao 266042, P. R. China.

[*]**Corresponding author:**

Prof. Dr. Xiliang Luo, Key Laboratory of Sensor Analysis of Tumor Marker Ministry of Education, College of Chemistry and Molecular Engineering, Qingdao University of Science and Technology, Qingdao 266042, P. R. China,

E-mail: xiliangluo@qust.edu.cn

Abstract

An aptamer induced "switch on" fluorescence resonance energy transfer (FRET) biosensor for the simultaneous detection of multiple tumor markers (e.g., AFP and CEA) combining molybdenum disulfide (MoS_2) nanosheets with multicolored Au NCs by a single excitation was developed for the first time. Here, AFP aptamer functionalized green colored Au NCs (510 nm) and CEA aptamer functionalized red colored Au NCs (650 nm) are used as energy donors, while MoS_2 is used as energy receptor. On the basis of recording the change of the recovered fluorescence intensity at 510 nm and 650 nm upon the addition of targets CEA and AFP, these two tumor markers can be simultaneously quantitatively detected, with detection limits of 0.16 and 0.21 ng mL^{-1} (3σ) for AFP and CEA, respectively. In addition, it is noteworthy that the developed biosensor can not only realize accurate quantitative determination of multiple tumor markers by fluorescent intensity, but also be applied in semi-quantitative determination through photo visualization. More importantly, confocal microscope experiments prove that serums from normal and hepatoma patients can also be visually and qualitatively discriminated by this FRET-based biosensor with a single excitation wavelength, indicating promising potential of this assay for clinical diagnosis.

Keywords Simultaneous detection; Single excitation; Biosensor; Tumor markers; Dual colored Au nanoclusters

1. Introduction

Highly sensitive and high-throughput sensing technologies for the detection of tumor markers are of great significance due to their versatile potential applications in early diagnosis and treatment for cancer [1]. Notably, many cancers are associated with multiple tumor markers, and the detection of a single tumor marker may cause false diagnosis which restricts diagnostic value in clinical analysis [2]. Simultaneous detection of multiple tumor markers, with the advantage of enhancing detection throughput, shortening analytical time and detection cost, can effectively improve the accuracy of early cancer diagnosis over the single marker assay. Currently, owing to the unique superiority of high sensitivity, convenience and low cost, a series of fluorescent techniques for multiple tumor marker analysis have been established [3-5]. In most cases, multiple lasers are needed to excite each fluorophore to collect the emissive fluorescence when multiple tumor marker are detected simultaneously. Thus, the background noise originating from multiple excitation wavelengths are difficult to be excluded, which inevitably restrict their clinical applications [6]. Therefore, simultaneous fluorescent detection of multiple tumor markers with a single excitation wavelength is highly desirable but remains a challenge.

Fluorescence resonance energy transfer (FRET), based on the nonradiative energy transfer from the fluorescent donor to the acceptor within short proximity (<10 nm), makes it possible for simultaneous detection of multiple tumor markers by recording emission intensities at different wavelengths with single excitation [7]. Until now, a series of FRET nanosensors have been developed to accomplish separate detection of diverse tumor markers with organic dyes or semiconductor quantum dots (QDs) as energy donors [8,9]. However, their practical application is limited owing to the non-negligible shortcomings, such as easy photo bleaching and poor

photo stability for organic dyes as well as high toxicity for QDs. Compared with organic dyes or QDs, gold nanoclusters (Au NCs) have been widely utilized in biosensing and bio-imaging due to their excellent biocompatibility, stable fluorescent emitting and good photo stability in the past few decades [10-14]. In addition, their size-dependent emission spectra make them good candidates for simultaneous excitation at a single wavelength [15]. Therefore, it is expected that FRET biosensors for the detection of multiple tumor markers may be developed using different colored Au NCs as energy donors, and more interestingly, these multicolored Au NCs may possibly be excited by a single wavelength. In addition, owing to the strong fluorescence quenching ability and high affinity to single-stranded DNA [16], molybdenum disulfide (MoS_2) nanosheets are considered to be promising fluorescent quencher candidates for the preparation of FRET-based aptasensors platforms. In 2013, Zhang's group firstly revealed the high fluorescence quenching ability of MoS_2 nanosheet for fluorescent dye labelled ssDNA [17]. After that, MoS_2 nanosheet based FRET biosensors for tumor markers detection have been developed, including epithelial cell adhesion molecule [18], DNA [19], DNA methyltransferase (MTase) activity [20] and thrombin [21] et al. Nevertheless, although MoS_2 have great potentials in FRET-based aptasensors, their integration with multicolored Au NCs for the development of aptasensor for simultaneous detection of multiple targets has not been explored.

In this work, we report a novel aptamer induced "switch on" FRET biosensor for simultaneous detection of multiple tumor markers using dual colored Au NCs as energy donors with a single excitation wavelength. As shown in **Scheme 1**, simultaneous detection of multiple tumor markers (e.g., AFP and CEA) are performed in the following procedure. Firstly, AFP aptamer functionalized green colored Au NCs (510 nm) and CEA aptamer functionalized red colored Au

NCs (650 nm) are simultaneously assembled onto the surface of MoS_2 nanosheets through van der Waals force. Thus, the fluorescence of the dual colored Au NCs was simultaneously quenched through static quenching due to the strong fluorescence quenching ability of MoS2 nanosheets. Secondly, upon the addition of the target tumor markers (AFP and CEA), green and red fluorescence will be simultaneously recovered along with the releasing of the two aptamer functionalized Au NCs, because of the higher affinity between aptamer and target tumor markers [22,23]. Therefore, simultaneous detection of multiple tumor markers can be achieved by monitoring the change of the recovered fluorescence intensity at 510 nm and 650 nm with a single excitation. Compared with the tranditional methods for simultaneous detection, several obvious advantages of this sensor array make it particularly attractive: (1) the biggest advantage of our present method is that multiple tumor markers could be simultaneously detected by a single excitation wavelength. (2) dual colored Au NCs with lower toxicity were firstly used as energy donors instead of semiconductor quantum dots, showing better biocompatibility. More importantly, the determination of multiple tumor markers can be achieved not only by recording fluorescence recovery intensity but also by photo visualization. Furthermore, serums from normal and hepatoma patients can also be visually discriminated by this FRET-based biosensor using single excitation wavelength, showing feasible potential for diagnostic applications.

2. Materials and methods

2.1. Materials

$HAuCl_4 \cdot 3H_2O$ (Hydrogen tetrachloroaurate trihydrate), carcinoembryonic antigen (CEA), α-fetoprotein (AFP), 11-mercaptoundecanoic acid (MUA), MoS_2 nanosheets and tetrakis

(hydroxymethyl) phosphonium chloride (THPC), Glutathione (GSH), bovine serum albumin (BSA),1-ethyl-3-(3-dimethylaminopropyl)carbodiimide hydrochloride (EDC), and N-hydroxylsuccinimide sodium salt (NHS) were purchased from Sigma-Aldrich (USA). All solutions were prepared using ultrapure water from a Millipore Simplicity 185 water purification system (Millipore, USA). DNA aptamers wwere purchased from Shanghai Sangon Biotechnology (Shanghai, China), and their sequences are as follows: AFP aptamer, 5'-GGCAGGAAGACAAACAAGCTTGGCGGCGGGAAGGTGTTTAAATTCCCGGGTCTGC GTGGTCTGTGGTGCTGT-NH_2-3'; CEA aptamer, 5′-ATACCAGCTTATTCAATT-NH_2-3'. Serum samples were obtained from the Eighth Peoples' Hospital of Qingdao, and they were collected with informed consent from the human subject. In addition, the sample collection was approved by Institutional Review Board of Eighth Peoples' Hospital of Qingdao. All reagents were of analytical reagent grade.

2.2. Instruments

The morphologies of all samples were characterized by a JEM-2100 transmission electron microscope (TEM) with an accelerating voltage of 200 kV. Fluorescence spectra were recorded by an F-4600 fluorescence spectrometer. Zeta potential experiments were performed with a Zetasizer Nano-ZS (Malvern Instruments, Malvern, UK). Infrared (IR) spectra were recorded using a FT/IR-410 Fourier transform infrared spectrophotometer (JASCO, Japan). Confocal images were collected with a Olympus FV1000 with excitation wavelength at 405 nm.

2.3. Synthesis of green emitting Au NCs (510 nm) and red emitting Au NCs (650 nm)

Green emitting Au NCs (510 nm) and red emitting Au NCs (650 nm) were prepared according to previous reports with some modifications [24,25]. In a typical synthesis experiment, all glass bottles were washed with aqua regia and rinsed with ultrapure water. For the synthesis of green emitting Au NCs, firstly, 6.0 μL 80% THPC and 250 μL 1.0 M NaOH were added to 20 mL ultrapure water. The mixture was stirred for 5 minutes, and then 1.0 mL 20 mM $HAuCl_4$ was quickly added to the mixture. The color of the solution changes from light yellow to brown within 60s. Then, 100 μL 117.5 mM GSH was added to obtain GSH protected Au nanoparticles. After stirring for another 15 minutes at room temperature, the solution was transferred to 4 °C for one day. Secondly, 2.0 mL stock Au nanoparticles solution was mixed with 400 μL 0.1 M PBS of pH 9.0 and 150 μL 0.1 M MUA ethanol solution for 2 h, and green emitting Au NCs (510 nm) were then obtained. For the synthesis of red emitting Au NCs, a solution of 50 mg mL-1 BSA was added to an equal volume of 10 mM $HAuCl_4$, and the pH of the resulting solution was adjusted to 12 by adding NaOH solution. The reaction was allowed to proceed under vigorous stirring at 37 °C overnight, and red emitting Au NCs (650 nm) were then obtained.

2.4. Preparation of AFP aptamer-Au NCs (510 nm) and CEA aptamer-Au NCs (650 nm)

For the preparation of the AFP aptamer-Au NCs (510 nm), 10 μL of green emitting Au NCs were added to 190 μL of PBS (pH 7.4), and then EDC (0.56 mg) and NHS (0.32 mg) were added to the proceeding solution at 37 °C with continuous vibration. After 30 min activation, 20 μL of 10 μM AFP aptamer was added into the above mixture. The condensation reaction was kept at

37 °C overnight. For the preparation of the CEA aptamer-Au NCs (650 nm), 4 μL of red emitting Au NCs were added to 196 μL of PBS (pH 7.4), and then EDC (0.56 mg) and NHS (0.32 mg) were added to the proceeding solution at 37 °C with continuous vibration. After 30 min activation, 20 μL of 10 μM CEA aptamer was added into the above mixture, and the condensation reaction was kept at 37 °C overnight.

2.5. Simultaneous detection of CEA and AFP

100 μL of CEA aptamer-Au NCs (650 nm) and 100 μL of AFP aptamer-Au NCs (510 nm) were mixed, and then 10 μL of 0.8 mg mL^{-1} MoS_2 nanosheets was introduced into the mixture at room temperature to quench the fluorescence with 20 min of incubation. Then, the recovered fluorescence was recorded in the presence of different concentrations of CEA (0, 0.5, 5, 15, 30, 60, 120, 150, 200 ng mL^{-1}) and AFP (0, 0.5, 5, 15, 30, 60, 120, 150, 200 ng mL^{-1}) after incubation for 30 min at 37 °C.

3. Results and discussion

3.1 Characterization of AFP aptamer-Au NCs (510 nm) and CEA aptamer-Au NCs (650 nm)

CEA aptamer and AFP aptamer were modified on the Au NCs (650 nm) and Au NCs (510 nm) by the condensation reaction with EDC/NHS, respectively. According to the spherical Jellium model [26], the fluorescent color of the AuNCs depends on their atomic composition (e.g., green for Au_{13} and red for Au_{25} emission). And accordance to the reviewer's suggestion, we have added matrix-assisted laser desorption/ionization-time of flight mass spectrometry (MALDI-TOF MS) to confirm the atomic composition of the GSH protected AuNCs and BSA protected AuNCs. As

shown in **Fig. S1A**, multipule peaks ascribed to the fragmentation of GSH protected Au NCs were observed with spacing of *m/z* 197. The maximum mass peak was observed at *m/z* 2561. Atomic weight of Au is 197, therefore, molecular weight of Au_{13} cluster is 2561. These peaks occurring at *m/z* 1576 (Au_8), 1773 (Au_9), 1970 (Au_{10}), 2167 (Au_{11}) and 2364 (Au_{12}) are considered as fragmented Au_{13} nanoclusters. This result suggested the formation of GSH protected Au_{13} nanoclusters. Similarly, **Fig. S1B** indicated the formation of BSA protected Au_{25} nanoclusters. We used the UV absorption to roughly estimate the modification efficiency of the aptamer onto Au NCs. After the reaction between aptamers and Au NCs, the incubation solution was filtrated with a 10 KDa ultrafiltration tube at 8000 rpm. Thus, the uncombined aptamers were into the filtrate. By comparing the concentration of aptamers in original solution and filtrate with UV absorption (**Fig. S2**), the modification efficiency of the aptamers onto Au NCs were roughly estimated to be 64.2% for AFP aptamer-Au NCs (510 nm) and 60.9% for CEA aptamer-Au NCs. Considering the modification efficiency of the AFP aptamers onto GSH protected Au NCs were roughly estimated to be 64.2% , 1.284×10^{-10} mol AFP aptamers were modified onto the GSH protected Au NCs. In other words, 2.755×10^{-4} mol AFP aptamers were modified onto 1 mol GSH protected Au NCs. Similarly, the final concentration of BSA protected Au NCs used for CEA aptamer modification was 1.9×10^{-8} mol. Considering the modification efficiency of the CEA aptamers onto BSA protected Au NCs were roughly estimated to be 60.9% , 1.218×10^{-10} mol CEA aptamers were modified onto the BSA protected Au NCs. In other words, 6.4×10^{-3} mol CEA aptamers were modified onto 1 mol BSA protected Au NCs. TEM images in **Fig. 1A** and **B** clearly show that the modified Au NCs are adsorbed onto the surface of MoS_2 nanosheets through van der waals force [16, 27]. Evidence for chemical modification was

further confirmed by FT-IR spectroscopy. By comparing the FT-IR spectra (**Fig. 1C** and **D**), it was concluded that the absorption intensity of the indicative peaks at 1555 cm^{-1} and 1626 cm^{-1}, which are ascribed to the N-H deformation and C=O stretching vibration, were obviously increased, suggesting the successful attachment of AFP aptamer and CEA aptamer on the surface of Au NCs (510 nm) and Au NCs (650 nm), respectively [28,29]. Additionally, the decreased zeta potentials of aptamer functionalized Au NCs (Here, the aptamer functionalized AuNCs which were used for zeta potential measurement had already been purified by a 10 KDa ultrafiltration tube) after the modification further confirmed the surface functionalization (**Fig. S3**). In a word, the TEM, FTIR and zeta potential confirm that CEA aptamer and AFP aptamer were successfully modified onto the surface of Au NCs (650 nm) and Au NCs (510 nm), respectively.

3.2 Selecting excitation wavelength and optimizing experimental conditions

For a typical simultaneous detection of multiple tumor markers experiment, multiple emission wavelength excited by a single excitation will greatly reduce the background noise as well as improve sensitivities than by multiple excitations [6]. As shown in **Fig. 2**, there is an overlapping region between the excitation spectra of the Au NCs (510 nm) and Au NCs (650 nm). That is to say, Au NCs (510 nm) and Au NCs (650 nm) could be simultaneous excited by any wavelength in this cross area. Considering the excitation efficiency for the two colored Au NCs, 430 nm was selected as the optimum excitation wavelength in the following experiments. Furthermore, it is worth noting that the emission spectrum of Au NCs (510 nm) separates well from that of Au NCs (650 nm), guaranteeing the subsequent accomplishment of simultaneous detection of two

tumor markers. In addition, the amounts of added MoS_2 nanosheets and the incubation time for fluorescence quenching were optimized. As shown in **Fig. S4**, 38.10 μg mL^{-1} of MoS_2 nanosheets and 20 min of incubation time were selected in the following experiments.

3.3 Simultaneous detection of AFP and CEA

The degree of fluorescence recovery is directly related to the concentration of the target tumor markers. Therefore, the AFP and CEA concentration can be monitored by tracking the recovered fluorescence signal at wavelengths of 510 nm and 650 nm. As shown in **Fig. 3**, with the increasing concentration of AFP and CEA, the fluorescence intensities at 510 nm and 650 nm simultaneously increased with excellent linear correlations, respectively. It was concluded that the fluorescence intensity increased linearly with the concentration of AFP from 0.5 to 60 ng mL^{-1} with a detection limit of 0.16 ng mL^{-1}, whereas CEA can be quantified within a linear range from 0.5 to 120 ng mL^{-1} with a detection limit of 0.21 ng mL^{-1}. We noticed that there is a little blue shift on the emission of Au NCs (650 nm) in the detection assays. the maximum emission wavelength of the red fluorescent Au NCs is 650 nm with the maximum excitation wavelength of 500 nm. However, in order to simultaneous excited Au NCs (510 nm) and Au NCs (650 nm) by a single wavelength with optimal excitation efficiency, 430 nm was selected as the excitation wavelength in the following detection assays. This might be the major reason for the blue shift on the emission of Au NCs (650 nm) in the detection assays. As a new AFP and CEA sensing approach, the limited detections the proposed assay is comparable to, or even better than, those of previously reported approaches for AFP and CEA detection [30-33]. To further expand the potential practical application of this proposed method, the recovery rates of different

concentrations of AFP and CEA in human serum were detected. We selected three final AFP concentrations (10, 30 and 60 ng/mL) and CEA concentrations (20, 60 and 100 ng/mL), which are in their corresponding liner range (0.5 to 60 ng/mL for AFP and 0.5 to 120 ng/mL for CEA) for the real sample test. As shown in **Table S1** in the supporting information, the recoveries were acceptable, ranging from 98.17% to 102.14% for AFP and 95.87% to 100.68% for CEA, indicating this proposed method could be applied to the quantitative detection of real samples.

It is noteworthy that visualization detection can also be evidently realized by this system. **Fig. 4** shows the photos of semi-quantitative determination of AFP and CEA, respectively and simultaneously (under UV illumination). When AFP was added to the fluorescent quenched solution, the recovered green color increased rapidly with increasing the concentration of AFP (**Fig. 4A**). Likewise, When CEA was added to the fluorescent quenched solution, the recovered red color increased rapidly with increasing the concentration of CEA (**Fig. 4B**). If both AFP and CEA were added to the fluorescent quenched solution, the fluorescence emission of the two distinguishing colored Au NCs (510 nm) and Au NCs (650 nm) increased simultaneously, and the solution exhibited their mixed color (**Fig. 4C**).

3.4 Cross-reaction analysis and selectivity

It is of high significance to eliminate cross-reactivity between analytes for simultaneous multiple analyte detection. Therefore, we investigated the degree of cross-reactivity between AFP and CEA by comparing the recovered fluorescence at 510 nm and 650 nm, respectively. As shown in **Fig. 5A**, when AFP alone was added to the quenched solution, increasing green fluorescence emission at 510 nm was observed. In contrast, when CEA alone was added to the

quenched solution, only red fluorescence emission at 650 nm was increased (**Fig. 5B**). These results demonstrated that the cross-reactivity between the two analytes was negligible.

Furthermore, the capability of resisting interference over potentially competing species is a requirement for an application in biomedical systems. To characterize the specificity of the developed biosensor, the selectivity of the biosensor to APF and CEA over some possible interferents (100 μg mL^{-1} of Pep, Lys, CAT, Try, Tf, HSA and BSA) was evaluated under the same conditions. As shown in **Fig. 5C**, the influence from the interferents on the recovered fluorescence intensity was negligible, demonstrating excellent specificity of the assay for CEA and AFP.

3.5 Visual discrimination between serums from hepatoma patients and healthy people

In order to further explore the application of the FRET biosensor to real samples, it was used to distinguish between serums from hepatoma patients and healthy people. Here, serums from hepatoma patients have already been diagnosed by the standard method of chemiluminescent microparticle immunoassay. Serums from healthy people and hepatoma patients (20 μL) were added to 200 μL of MoS_2 nanosheets quenched AFP aptamer-Au NCs (510 nm) and CEA aptamer-Au NCs (650 nm) mixtures at 37 °C, respectively. After 30 minutes, confocal microscope images demonstrate the prominent differences. As shown in **Fig. 6**, green and red fluorescent colors were clearly observed when serums from hepatoma patients were added into the quenched mixtures, whereas almost no significant recovered fluorescence was observed when serums from healthy people were added. Although the Au NCs aggregated for a certain degree, the recovered fluorescence was hardly affected as shown in **Fig S5**. Clinically, the content of certain proteins (especially AFP and CEA) in the serum of hepatoma patients will be

significantly increased compared with those of the healthy people [34-36]. Therefore, this well visual discrimination was resulted from the increasing concentration of AFP and CEA in hepatoma patients' serums. Consequently, the FRET biosensor can offer an auxiliary method for the clinical standard method to discriminate between hepatoma patients and healthy people, demonstrating great beneficial for the clinical diagnosis of liver cancer.

4. Conclusions

In summary, a simple and sensitive aptamer-induced "switch on" FRET biosensor for simultaneous detection of multiple tumor markers with dual-color fluorescence output signals was developed. The two contrasting colored fluorescence signals can be simultaneously monitored without spectra overlap by a single excitation, and the simultaneous detection of APF and CEA can be easily realized. In addition, semi-quantitative determination of AFP and CEA by photo visualization can also be realized. More importantly, it was also successfully applied to visually distinguish between serums from hepatoma patients and healthy people, showing great beneficial for the clinical diagnosis. The present study provided a new method for simultaneous detection of multiple tumor markers, and it is expected that it may greatly contribute to disease diagnostics and other biosensor applications.

Acknowledgements

The authors gratefully acknowledge the support from the National Nature Science Foundation of China (21422504, 21505081, 21675093), the Natural Science Foundation of Shandong Province of China (JQ201406), the Doctoral Found of QUST and the Taishan Scholar Program of Shandong Province, China.

Reference

[1] D.A. Giljohann, C.A. Mirkin, Drivers of biodiagnostic development, Nature 462 (2009) 461-464.

[2] T.M. Nascimento, G.G. Morbioli, L.A. Milan, F.C. Donofrio, C.A. Mestriner, E. Carrilho, Development and statistical assessment of a paper-based immunoassay for detection of tumor markers, Anal. Chim. Acta. 950 (2017) 156-161.

[3] A. Beharry, S. Lacoste, T. Connor, E.T. Koo, Fluorescence Monitoring of the Oxidative Repair of DNA Alkylation Damage by ALKBH3, a Prostate Cancer Marker, J. Am. Chem. Soc. 138 (2016) 3647-3650.

[4] W.B. Liang, C.C.Fan, Y. Zhuo, Y.N. Zheng, C.Y. Xiong, Y.Q. Chai, R. Yuan, Multiparameter Analysis-Based Electrochemiluminescent Assay for Simultaneous Detection of Multiple Biomarker Proteins on a Single Interface, Anal. Chem. 88 (2016) 4940-4948.

[5] W.H. Zhang, W. Ma, Y.T. Long, Redox-Mediated Indirect Fluorescence Immunoassay for the Detection of Disease Biomarkers Using Dopamine-Functionalized Quantum Dots, Anal. Chem. 88 (2016) 5131-5136.

[6] W. Pan, Y.L. Li, M.M. Wang, H.J. Yang, N. Li, B. Tang, FRET-based nanoprobes for simultaneous monitoring of multiple mRNAs in living cells using single wavelength excitation, Chem. Commun. 52 (2016) 4569-4572.

[7] M. Wu, E. Petryayeva, W. Algar, Quantum dot-based concentric FRET configuration for the parallel detection of protease activity and concentration, Anal. Chem. 86 (2014) 11181-11188.

[8] W.B. Qiang, W. Li, X.Q. Li, X. Chen, D.K. Xu, Bioinspired polydopamine nanospheres: a superquencher for fluorescence sensing of biomolecules, Chem. Sci. 5 (2014) 3018-3024.

[9] Y.H. Wang, D.Y. Gao, P.F. Zhang, P. Gong, C. Chen, G.H. Gao, L.T. Cai, A near infrared fluorescence resonance energy transfer based aptamer biosensor for insulin detection in human plasma, Chem. Commun. 50 (2014) 811-813.

[10] C.Q. Ding, Y. Tian, Gold nanocluster-based fluorescence biosensor for targeted imaging incancer cells and ratiometric determination of intracellular pH, Biosens. Bioelectron. 65 (2015) 183-190.

[11] S.H. Xu, X.Y. Feng, T. Gao, R.Z. Wang, Y.N. Mao, J.H. Lin, X.J. Yu, X.L. Luo, A novel dual-functional biosensor for fluorometric detection of inorganic pyrophosphate and pyrophosphatase activity based on globulin stabilized gold nanoclusters, Anal. Chim. Acta. 958 (2017) 22-29.

[12] S.H. Xu, X. Lu, C.X. Yao, F. Huang, H. Jiang, W.H. Hua, N. Na, H.Y. Liu, J. Ouyang, A visual sensor array for pattern recognition analysis of proteins using novel blue-emitting fluorescent gold nanoclusters, Anal. Chem. 86 (2014) 11634-11639.

[13] S.H. Xu, T. Gao, X.Y. Feng, Y.N. Mao, P.P. Liu, X.J. Yu, X.L. Luo, Dual ligand co-functionalized fluorescent gold nanoclusters for the “turn on” sensing of glutathione in tumor cells, J. Mater. Chem. B 4 (2016) 1270-1275.

[14] X.M. Yang, Y.W. Luo, Y. Zhuo, Y.J. Feng, S.S. Zhu, Novel synthesis of gold nanoclusters templated with l-tyrosine for selective analyzing tyrosinase, Anal. Chim. Acta. 840 (2014) 87-92.

[15] L.Y. Chen, C.W. Wang, Z.Q. Yuan, H.T. Chang, Fluorescent Gold Nanoclusters: Recent Advances in Sensing and Imaging, Anal. Chem. 87 (2015) 216-229.

[16] C.F. Zhu, Z.Y. Zeng, H. Li, F. Li, C.H. Fan, H. Zhang, Single-layer MoS_2-based nanoprobes for homogeneous detection ofniomolecules, J. Am. Chem. Soc. 135 (2013) 5998-6001.

[17] C.F. Zhu, Z.Y. Zeng, H. Li, F. Li, C.H. Fan, H. Zhang, Single-Layer MoS_2-Based Nanoprobes for Homogeneous Detection of Biomolecules, J. Am. Chem. Soc. 30 (2008) 5998-6001.

[18] J.Y. Shi, J. Lyu, F. Tian, M. Yang, A fluorescence turn-on biosensor based on graphene quantum dots (GQDs) and molybdenum disulfide (MoS2) nanosheets for epithelial cell adhesion molecule (EpCAM) detection, Biosens. Bioelectron. 93 (2017) 182-188.

[19] J.H. Huang, L. Ye, X. Gao, H. Li, J.B. Xu, Z.G. Li, Molybdenum disulfide-based amplified fluorescence DNA detection using hybridization chain reactions, J. Mater. Chem. B 3 (2015) 2395-2401.

[20] H.M. Deng, X.J. Yang, Z.Q. Gao, MoS_2 nanosheets as an effective fluorescence quencher for DNA methyltransferase activity detection, Analyst 140 (2015) 3210-3215.

[21] J. Ge, E.C. Ou, R.Q. Yu, X. Chu, A novel aptameric nanobiosensor based on the self-assembled DNA–MoS2 nanosheet architecture for biomolecule detection, J. Mater. Chem. B 2 (2014) 625-628.

[22] C. Tuerk, L. Gold, Systematic evolution of ligands by exponential enrichment: RNA ligands to bacteriophage T4 DNA polymerase, Science 249 (1990) 505-510.

[23] A.D. Ellington, J.W. Szostak, In vitro selection of RNA molecules that bind specific ligands, Nature 346 (1990) 818-822.

[24] J.P. Xie, Y.G. Zheng, J.Y. Ying, Protein-directed synthesis of highly fluorescent gold nanoclusters, J. Am. Chem. Soc. 131 (2009) 888-889.

[25] Z.Q.Yuan, M.H. Peng, Y. He, E.S. Yeung, Functionalized fluorescent gold nanodots: synthesis and application for Pb^{2+} sensing, Chem. Commun. 47 (2011) 11981-11983.

[26] H. Kawasaki, K. Hamaguchi, I. Osaka, R. Arakawa, ph-Dependent Synthesis of Pepsin-Mediated Gold Nanoclusters with Blue Green and Red Fluorescent Emission, Adv. Funct. Mater. 21 (2011) 3508-3515.

[27] S. He, B. Song, D. Li, C. Zhu, W. Qi, Y. Wen, L. Wang, S. Song, H. Fang, C. Fan, A graphene nanoprobe for rapid, sensitive, and multicolor fluorescent DNA analysis, Adv. Funct. Mater. 20 (2010) 453-459.

[28] M.J. Liang, Y.L. Chen, H.J. Zhang, X.Y. Niu, L.F. Xu, C.L. Ren, X.G. Chen, Fluorescence resonance energy transfer-based ratiometric fluorescent assay for highly sensitive and selective determination of sulfide anions, Analyst 140 (2015) 6711-6719.

[29] M. Zhuang, C. Ding, A. Zhu, Y. Tian, Ratiometric fluorescence probe for monitoring hydroxyl radical in live cells based on gold nanoclusters, Anal. Chem. 86 (2014) 1829-1836.

[30] X.X. Liu, X.D. Song, Z.Y. Dong, X.T. Meng, Y.P. Chen, L. Yang, Photonic crystal fiber-based immunosensor for high-performance detection of alpha fetoprotein, Biosens. Bioelectron. 91 (2017) 431-435.

[31] H. Miao, L. Wang, Y. Zhuo, Z.N. Zhou, X.M. Yang, Label-free fluorimetric detection of CEA using carbon dots derived from tomato juice, Biosens. Bioelectron. 86 (2016) 83-89.

[32] C.Y. Wang, F. Hou, Y.C. Ma, Simultaneous quantitative detection of multiple tumor markers with a rapid and sensitive multicolor quantum dots based immunochromatographic test strip, Biosens. Bioelectron. 68 (2015) 156-162.

[33] Y.P. Chen, Y.L. Xianyu, J.S. Sun, Y.J. Niu, Y. Wang, X.Y. Jiang, One-step detection of pathogens and cancer biomarkers by the naked eye based on aggregation of immunomagnetic beads, Nanoscale 8 (2016) 1100-1107.

[34] J.M. Escudero, J.M. Auge, X. Filella, A. Torne, J. Pahisa, R. Molina, Comparison of serum human epididymis protein 4 with cancer antigen 125 as a tumor marker in patients with malignant and nonmalignant diseases, Clin. Chem. 57 (2011) 1534-1544.

[35] S.H. Xu, P.P. Liu, X. Lu, J. Zhang, L.Y. Huang, W.H. Hua, D.C. He, J. Ouyang, A highly sensitive “turn-on” fluorescent sensor for the detection of human serum proteins based on the size exclusion of the polyacrylamide gel, Electrophoresis 35 (2014) 546-553.

[36] X.M. Yang, Y. Zhuo, S.S. Zhu, Y.W. Luo, Y.J. Feng, Y. Xu, Selectively assaying CEA based on a creative strategy of gold nanoparticles enhancing silver nanoclusters' fluorescence, Biosens. Bioelectron. 64 (2015) 345-351.

Figure captions

Scheme. 1 Schematic illustration of the dual color FRET biosensor for simultaneous detection of multiple tumor markers.

Fig.1 (A) TEM image of MoS_2. (B) TEM and HRTEM images of AFP aptamer-Au NCs (510 nm) and CEA aptamer-Au NCs (650 nm) adsorbed on MoS_2. (C) FT-IR spectra of (a) the AuNCs(650nm)/CEA aptamer, (b) the AuNCs(650nm), (c) the AuNCs(650nm)/EDC-NHS and (d) the AuNCs(650nm)/EDC-NHS/CEA aptamer. (D) FT-IR spectra of (a) the AuNCs(510nm)/AFP aptamer, (b) the AuNCs(510nm), (c) the AuNCs(510nm)/EDC-NHS and (d) the AuNCs(510 nm)/EDC-NHS/AFP aptamer.

Fig. 2 Fluorescence excitation (black dashed line) and emission (green line) spectra of the Au NCs (510 nm), and fluorescence excitation (blue dotted line) and emission (red line) spectra of the Au NCs (650 nm). Inset shows the photographs of the Au NCs (510 nm) and Au NCs (650 nm) under UV light illumination.

Fig. 3 (A) Fluorescence spectra of the mixture of AuNCs(510 nm)/AFP aptamer, AuNCs(650nm)/CEA aptamer and MoS_2 nanosheets with increasing concentration of AFP and CEA. (B) Linear curve for AFP detection. (C) Linear curve for CEA

detection.

Fig. 4 Photograph of semi-quantitative determination of AFP and CEA, respectively, and simultaneously under UV illumination. (A) The fluorescence quenched mixtures added with various amounts of AFP (from left to right): 0, 30, 60, 120, 150, and 200 nM. (B) The fluorescence quenched mixtures added with various amounts of CEA (from left to right): 0, 15, 60, 120, 150, and 200 nM. (C) The fluorescence quenched mixtures added with various amounts of AFP and CEA. The concentrations of AFP were 200, 150, 120, 60, and 0 nM, and the concentrations of CEA were 0, 60, 120, 150, and 200 nM (from left to right).

Fig. 5 Fluorescence spectra of the recovered fluorescence with the increasing concentrations of (A) pure AFP and (B) pure CEA. (C) Influence of 100 μg mL^{-1} Pep, Lys, CAT, Try, Tf, HSA and BSA on the recovered fluorescence compared with that of AFP (100 ng mL^{-1}) and CEA (100 ng mL^{-1}).

Fig. 6 Laser confocal microscope images of MoS_2 quenched AFP aptamer-Au NCs (510 nm) and CEA aptamer-Au NCs (650 nm) mixtures in the presence of serums from (A) healthy people and (B) hepatoma patients.

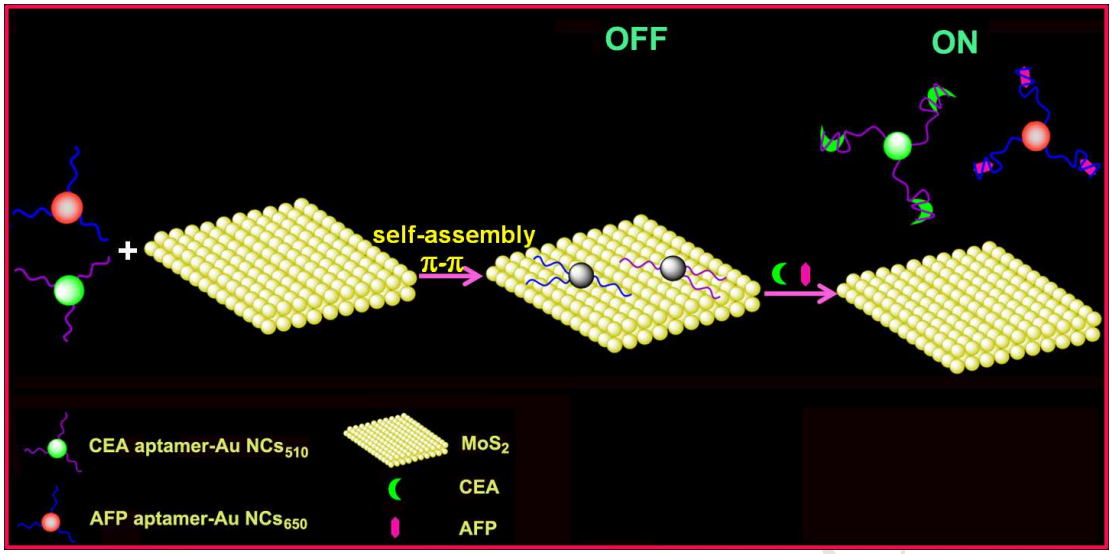

Scheme . 1

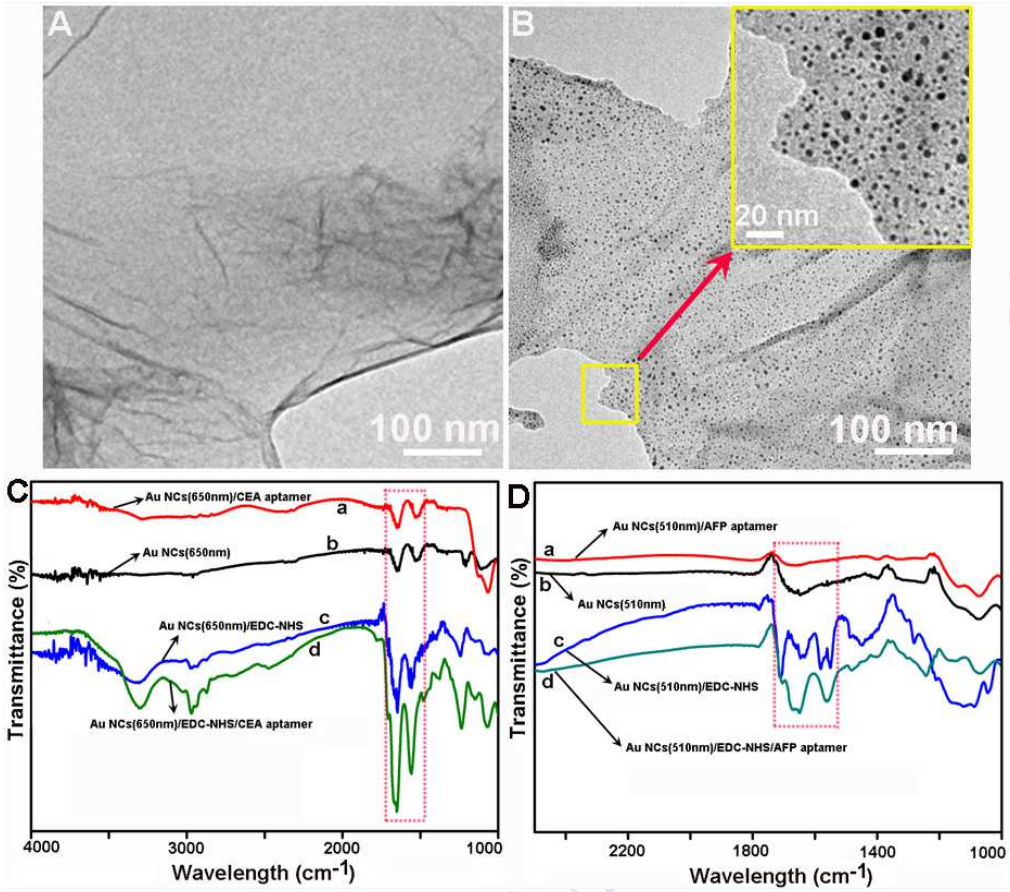

Fig. 1

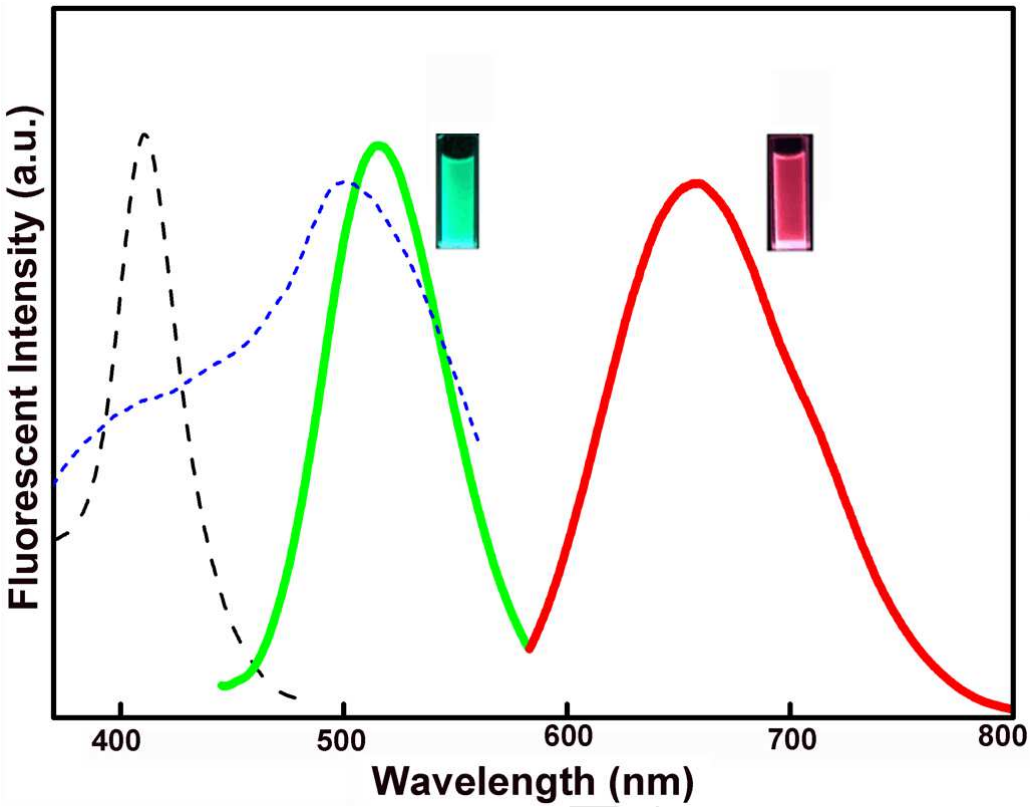

Fig. 2

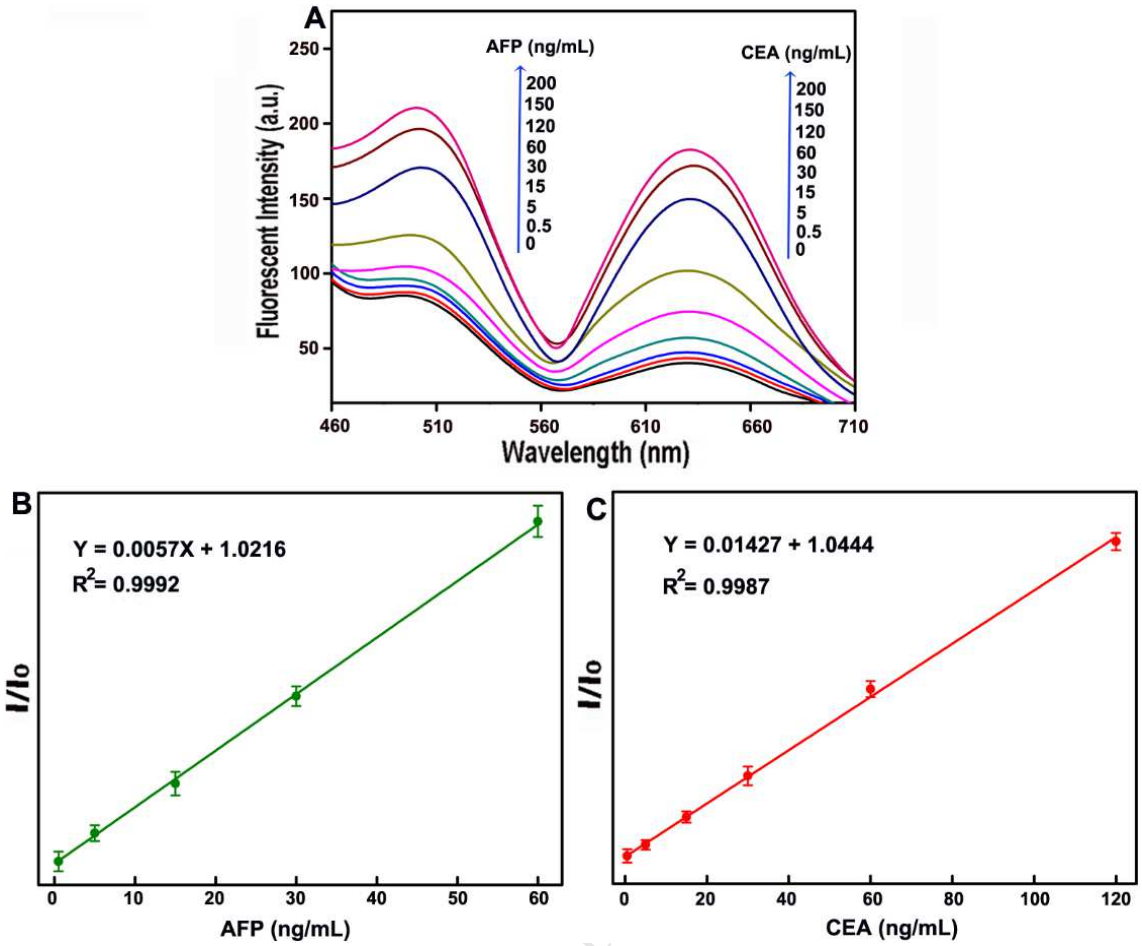

Fig. 3

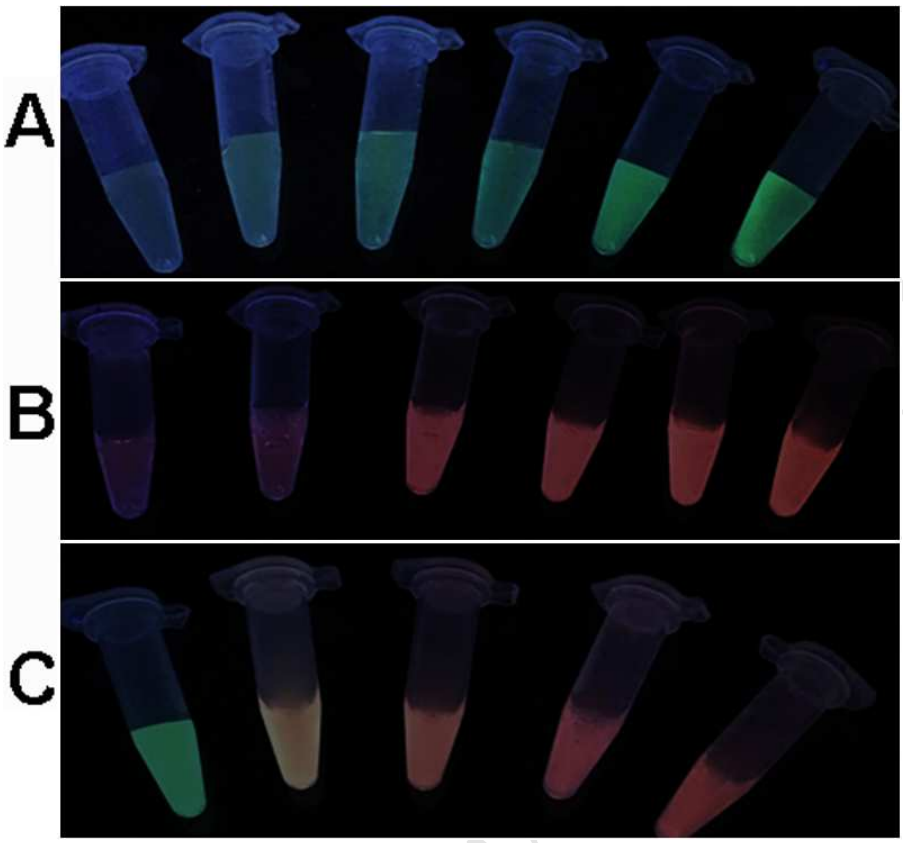

Fig. 4

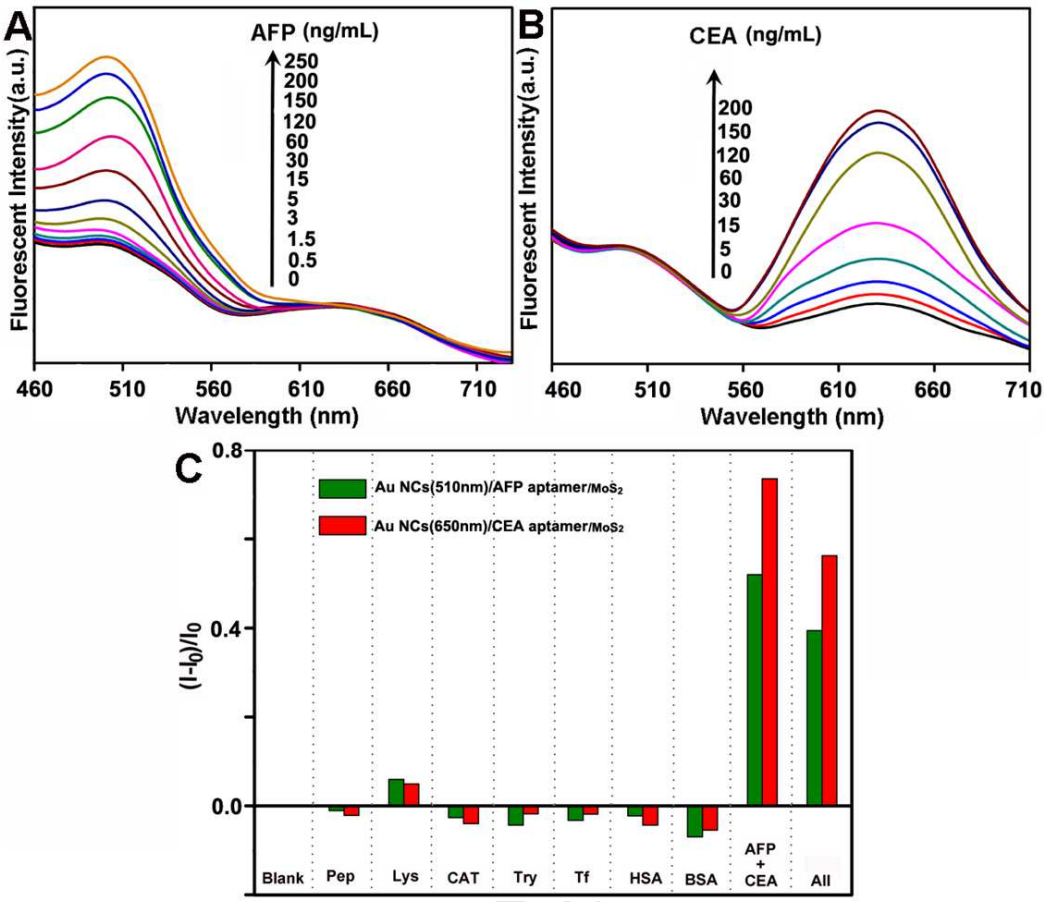

Fig. 5

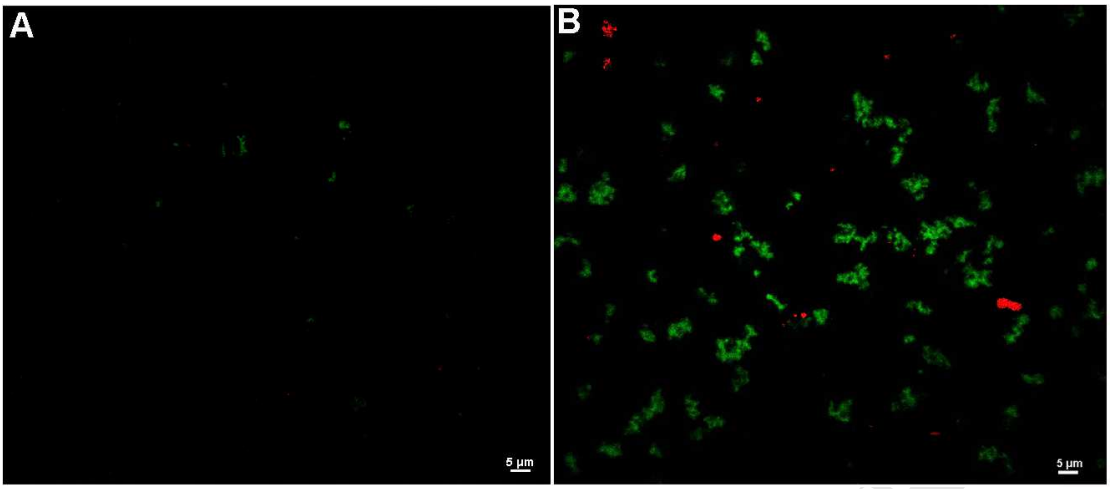

Fig. 6

Highlights:

► Dual colored Au NCs were used as energy donors of the FRET-based aptasensor for the first time

► Multiple tumor markers could be simultaneously detected with a single excitation

► Serums from normal and hepatoma patients could be visually discriminated by this FRET-based aptasensor